npj | vaccines

Article

Published in partnership with the Sealy Institute for Vaccine Sciences

https://doi.org/10.1038/s41541-024-00963-4

CircRNA based multivalent neuraminidase vaccine induces broad protection against influenza viruses in mice

Xinyu Yue[1,11], Cailing Zhong[2,11], Rui Cao[1,11], Sizhe Liu[1,11], Zhiran Qin[3], Lin Liu[1], Yanmei Zhai[1], Wanyu Luo[1], Yikai Lian[3], Mengjie Zhang[3], Hongjie Lu[1], Yuanyuan Wang[1], Mengxin Xu[1], Shuning Liu[1], Kexin Lv[1], Yuzhu Sun[1], Xingchen Zhu[1], Haoting Mai[1], Jing Liao[4], Jingyi Yang[5], Lei Deng[6], Yang Liu[3], Caijun Sun[1], Ke-Wei Zheng[7] ✉, Yuelong Shu[1,8] ✉ & Yao-Qing Chen[1,9,10] ✉

Developing broad-spectrum influenza vaccines is crucial for influenza control and potential pandemic preparedness. Here, we reported a novel vaccine design utilizing circular RNA (circRNA) as a delivery platform for multi-subtype neuraminidases (NA) (influenza A N1, N2, and influenza B Victoria lineage NA) immunogens. Individual NA circRNA lipid nanoparticles (LNP) elicited robust NA-specific antibody responses with neuraminidase inhibition activity (NAI), preventing the virus from egressing and infecting neighboring cells. Additionally, the administration of circRNA LNP induced cellular immunity in mice. To achieve a universal influenza vaccine, we combined all three subtypes of NA circRNA-LNPs to generate a trivalent circRNA vaccine. The trivalent vaccine elicited a balanced antibody response against all three NA subtypes and a Th1-biased immune response in mice. Moreover, it protected mice against the lethal challenge of matched and mismatched H1N1, H3N2, and influenza B viruses, encompassing circulating and ancestral influenza virus strains. This study highlights the potential of delivering multiple NA antigens through circRNA-LNPs as a promising strategy for effectively developing a universal influenza vaccine against diverse influenza viruses.

Hemagglutinin (HA) and neuraminidase (NA) are the two major glycoproteins on the influenza envelope. NA is the second most abundant glycoprotein on the influenza virus envelope and promotes virus release during the influenza replication cycle[1,2]. The current effectiveness of the influenza vaccine is primarily demonstrated by its ability to induce hemagglutination inhibition antibody responses. However, seasonal influenza viruses often exhibit significant immune evasion against such immune responses. In recent years, there has been increasing recognition of the crucial role of NA-specific immunity in conferring cross-protection[1–3]. NA has a slower mutation rate than HA proteins, which are prone to rapid antigenic drift[4]. Our previous work revealed that natural influenza virus infection induces a significant proportion of NA-reactive B cells and broadly neutralizing NA antibodies in humans[5]. These NA-reactive antibodies demonstrated robust NA inhibitory activity in vitro, protecting mice from lethal challenge.

[1]School of Public Health (Shenzhen), Shenzhen Campus of Sun Yat-Sen University, Shenzhen, China. [2]School of Pharmaceutical Sciences, Shenzhen Campus of Sun Yat-Sen University, Shenzhen, China. [3]Institute of Infectious Disease, Shenzhen Bay Laboratory, Shenzhen, Guangdong, China. [4]GMU-GIBH Joint School of Life Sciences, Guangzhou Medical University, Guangzhou, China. [5]Vaccine and Immunology Research Center, Translational Medical Research Institute, Shanghai Public Health Clinical Center, Fudan University, Shanghai, China. [6]Hunan Provincial Key Laboratory of Medical Virology, College of Biology, Hunan University, Changsha, China. [7]School of Biomedical Sciences, Hunan University, Changsha, China. [8]Key Laboratory of Pathogen infection prevention and control (Peking Union Medical College, Ministry of Education), State Key Laboratory of Respiratory Health and Multimorbidity, National Institute of Pathogen Biology of Chinese Academy of Medical Science (CAMS)/ Peking Union Medical College (PUMC), Beijing, China. [9]Key Laboratory of Tropical Disease Control (Sun Yat-sen University), Ministry of Education, Guangzhou, China. [10]Shenzhen Key Laboratory of Pathogenic Microbes and Biosafety, Shenzhen, China. [11]These authors contributed equally: Xinyu Yue, Cailing Zhong, Rui Cao, Sizhe Liu. ✉e-mail: zhengkewei@hnu.edu.cn; shuylong@mail.sysu.edu.cn; chenyaoqing@mail.sysu.edu.cn

Additionally, recent studies have identified a large number of conserved neutralizing epitopes on NA[6–10]. Studies in guinea pigs and humans have shown that anti-NA immunity can hinder viral transmission[11–13]. Thus, NA could be a potential target for broad-spectrum influenza vaccine development.

However, licensed influenza vaccines have not sufficiently induced a robust NA-specific antibody response[5]. This may be attributed to the absence of sufficient NA components in the vaccines or their degradation during production. Attempts to address this challenge include incorporating recombinant NA protein into seasonal vaccines[14–16], manipulating viral packaging signals to increase NA content[17], and extending NA stalk length on the virus particles to enhance NA immunogenicity[18]. Notably, mRNA technology offers a unique advantage by delivering membrane-bound NA in their native conformation, which has shown promising results in inducing potent anti-NA immunity in mice[19,20]. Vaccination with an NA mRNA vaccine can induce NA-reactive antibodies, including NA inhibition (NAI), antibody-dependent cellular cytotoxicity (ADCC) antibodies, and cellular immune response[20–22].

Circular RNA (circRNA) is a class of covalently closed ring RNA molecules generated by RNA splicing in eukaryotic cells. CircRNA lacks exposed 3' and 5' ends, making it resistant to degradation by most nucleases. This stability provides an advantage over linear RNA, such as mRNA. Incorporating internal ribosome entry site (IRES) allows circRNA to facilitate long-lasting protein expression[23]. CircRNA vaccines encoding the receptor-binding domain (RBD) have demonstrated efficacy against SARS-CoV-2 variants (Delta and Omicron) in mice and rhesus monkeys[24]. In addition to stability, circRNA possesses potent adjuvant properties. They can effectively activate intracellular sensors like RIG-I and MDA5, promoting the maturation of dendritic cells (DCs) and triggering robust immune responses[25]. Studies have shown a rapid increase in proinflammatory factors and chemokines following circRNA injection, leading to significant recruitment of immune cells (DCs, monocytes, and macrophages) to the injection site. Long-lasting and robust T cell responses were observed in mice immunized with circRNA encoding OVA[25]. T cells targeting conserved epitopes can provide an additional layer of protection when the virus escapes antibodies[26–28]. These combined attributes position circRNA as a promising platform for developing next-generation, broadspectrum influenza vaccines.

Here, we designed circRNA vaccines containing N1, N2, and influenza B virus NA antigens to elicit broad-spectrum NA immunity against heterologous influenza. This trivalent circRNA vaccine successfully induced robust NA-specific humoral and cellular immunity in mice. Moreover, it protected mice against lethal challenges with homologous and heterologous strains of H1N1, H3N2, and Victoria lineage influenza B viruses. These findings provide compelling evidence that the NA-targeting circRNA vaccine holds considerable promise for achieving broad-spectrum protection against influenza in mice and can be considered a novel strategy for potential universal influenza vaccine development.

Results

Preparation and characterization of circRNA-NA Vaccines

NA from three circulating seasonal influenza vaccine strains were selected: A/Michigan/45/2015 (H1N1), A/Switzerland/9715293/2013 (H3N2), and B/Florida/12/2017 (Victoria) (Fig. 1a and Fig. S1). These strains were selected because they predominated in recent seasons. The vaccine did not include the Yamagata lineage virus NA as it has been rarely detected since 2020[29]. CircRNAs encoding the selected NAs were synthesized using the permuted intron-exon (PIE) splicing strategy and subsequently encapsulated into lipid nanoparticles (LNPs) via an iNanoE microfluidic system. Sanger sequencing confirmed accurate ligation of the circRNAs (Fig. 1b). Gel electrophoresis demonstrated that circRNA can resist the hydrolysis by RNase R. (Fig. 1c). All prepared LNPs exhibited consistent characteristics, with ~80 nm particle size and polydispersity indices (PDI) < 0.2. The encapsulation efficiency of these LNPs exceeded 93% (Fig. 1e).

To evaluate NA expression from circRNA, HEK293T cells were transfected with LNP-encapsulated circRNAs. The expression of NA antigens was confirmed by flow cytometry using a broad-spectrum NA antibody 1G01[10], an N2-specific antibody 229-2C06[5], or an influenza B virus NA-specific antibody CC61 (isolated and identified by Prof. Chen's laboratory). Analysis indicated stable NA expression in approximately 98% of transfected cells, indicating efficient protein translation from circRNAs (Fig. 1f). Furthermore, to verify whether the NA antigens produced by circRNA were functional, the cells transfected with circRNA-LNP were tested for NA activity using a 2′-(4-methylumbelliferyl)-α-D-N-acetylneuraminic acid (MUNANA) substrate. Positive enzyme activity confirmed the native conformation of NA antigens produced by circRNAs (Fig. 1d)[30].

CircRNA-NA vaccines elicited robust immunity in mice

To evaluate the immunogenicity of circRNA vaccines in mice, groups of mice ($n = 5$) were administered two doses (10 μg or 2 μg for each dose, respectively) of each circRNA-NA, with a four-week interval between doses (Fig. 2a). Antibody titers were assessed after primary and booster vaccinations, revealing all three vaccines elicited significant increases in NA-specific antibody levels compared to the control group in a dose-dependent manner (Fig. 2b–d). For all the groups, serum titers significantly increased after booster immunization, with most animals exceeding 10^4 (Fig. 2b–d). The binding breadth of immune sera indicated that monovalent vaccines could induce specific antibodies against heterologous NAs within the same NA subtype (Fig. 2e–g). Given the potential link correlation between NAI antibody titers and protection[13,31,32], NAI antibodies against homologous NA were evaluated. Boosting circRNA-NA administration significantly increased NAI titers (over 1000 or near 1000, except 2 μg dose in the N2 group, Fig. 2h–j). Suggesting that booster vaccination may be necessary to stimulate the maturation of NA-specific B cells and the production of functional antibodies. Therefore, a two-dose immunization regimen was adopted for subsequent studies.

To further assess vaccine efficacy, a microneutralization assay (MN assay) was conducted to evaluate the sera' capacity to inhibit virus replication in vitro. MN assay results confirmed that post-boost sera from all groups exhibited significant virus neutralization activity (Fig. 2k–m). Notably, the N2 groups demonstrated particularly strong neutralizing activity against the homologous A/Switzerland/9715293/2013 virus (MN titer ~1000, Fig. 2h). Since NA antibodies do not directly neutralize viral infection, it is plausible that the immune serum used in the MN experiments suppressed the virus by inhibiting viral release and subsequent infection of neighboring cells. Overall, the above data confirmed that circRNA vaccines containing NA antigens presented strong immunogenicity, inducing NAI and neutralizing antibodies in mice.

CircRNA-NA vaccine induced NA-specific T cell response in mice

In addition to eliciting robust humoral responses, cellular immunity was also instrumental in enhancing the protective efficacy of vaccines. Previous studies on nucleic acid vaccines, such as mRNA, have successfully induced antigen-specific T cell responses[33–35]. NA-specific T cell responses were evaluated by Enzyme-linked immunosorbent spot (ELISpot) assay. Results indicated that all three circRNA vaccines significantly increased the number of IFN-γ and IL-4 producing cells compared with the control group (Fig. 3a–e). These findings were further corroborated by intracellular cytokine staining (ICS) assays (Fig. 3f–h and Fig. S2).

Upon stimulation with recombinant N1, N2, or influenza B virus (IBV) NA proteins, $CD4^+$ T cells producing IFN-γ, TNF-α, and IL-2 were detected in mice that received the circRNA vaccine (Fig. 3f–h). IFN-γ-secreting $CD8^+$ T cells were detected in mice immunized with circRNA-N1 and circRNA-IBV-NA (Fig. 3f, h). The proportion of IFN-γ-secreting $CD8^+$ T cells was also observed in the group immunized with circRNA-N2, although there was no significant difference between the groups ($P = 0.078$) (Fig. 3g). Overall, these data demonstrate that the circRNA-NA vaccine can induce NA-specific T cell responses in mice, encompassing both $CD4^+$ and $CD8^+$ subsets.

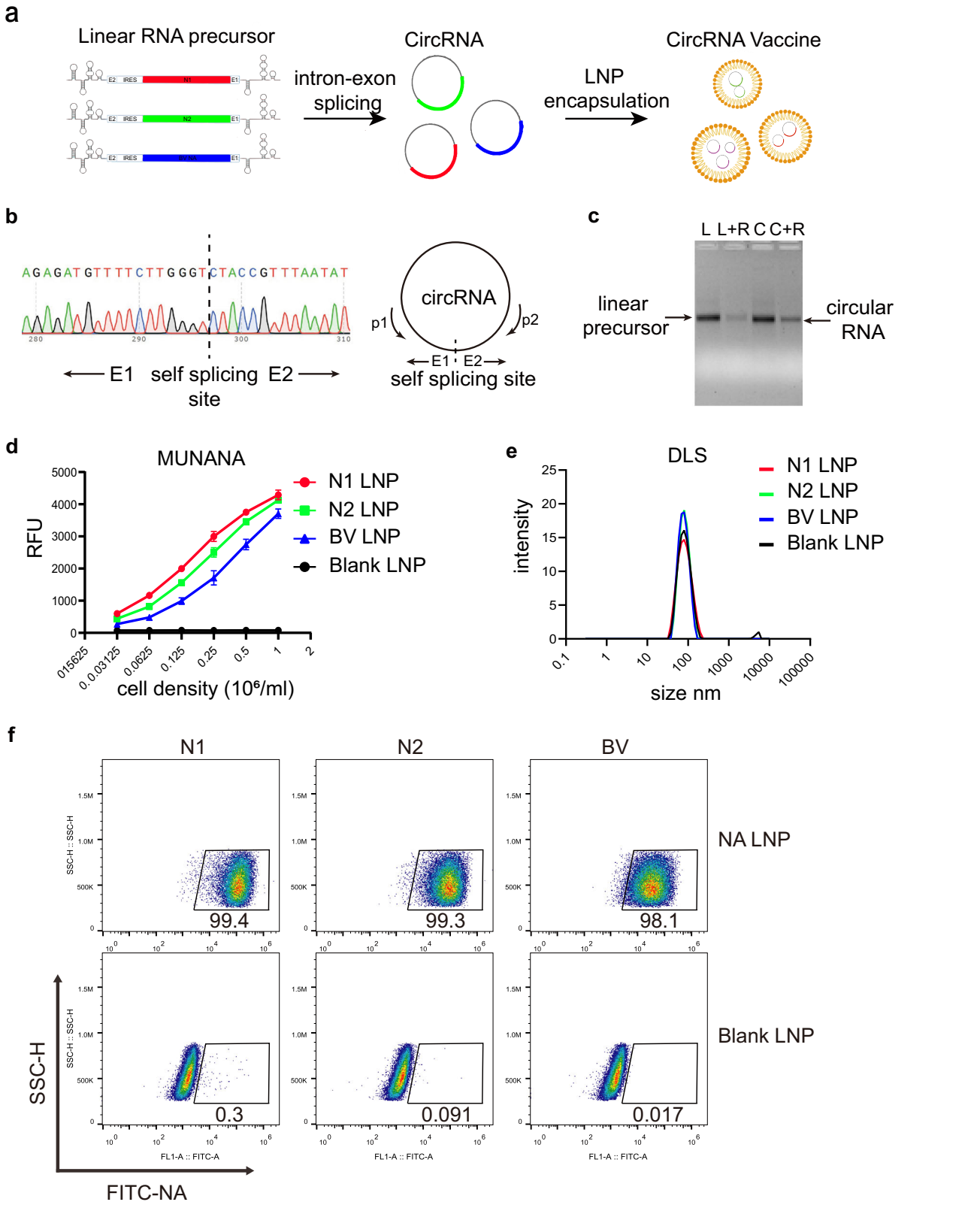

Fig. 1 | Design and characterization of circRNA-LNP encoding NA. a Schematic diagram of circRNA vaccine production. Linear RNA precursors encoding N1, N2, and IBV NA were self-spliced by group I catalytic intron to form circRNA. CircRNA was then encapsulated into lipid nanoparticles (LNP). The figure was created by the author using Adobe Illustrator 2020. **b** Verify the self-splicing junction site of circRNA using Sanger sequencing of the junction site after reverse transcription and PCR amplification. **c** CircRNA and linear precursor were separated on 1.5% agarose gel. Lane L: Linear precursor. Lane L + R: Linear precursor digested with RNase R. Lane C: circRNA not digested with RNase R. Lane C + R: circRNA digested with RNase R. **d** MUNANA assay for measuring NA enzyme activity in LNP-transfected cells. The curve shows the fluorescence intensity versus the density of cells in 50 μL. Data was shown as means of four repeated experiments ± SD. **e** Dynamic light scattering (DLS) to characterize the particle size and dispersion of circRNA-LNP. Representative images of each LNP were shown. **f** Frequency of NA expression in 293 T cells transfected with NA LNP, Blank LNP as a negative control. IRES: internal ribosome entry site. E1: exon fragment 1 upstream of 5'intron. E2: exon fragment 2 downstream of 3'intron.

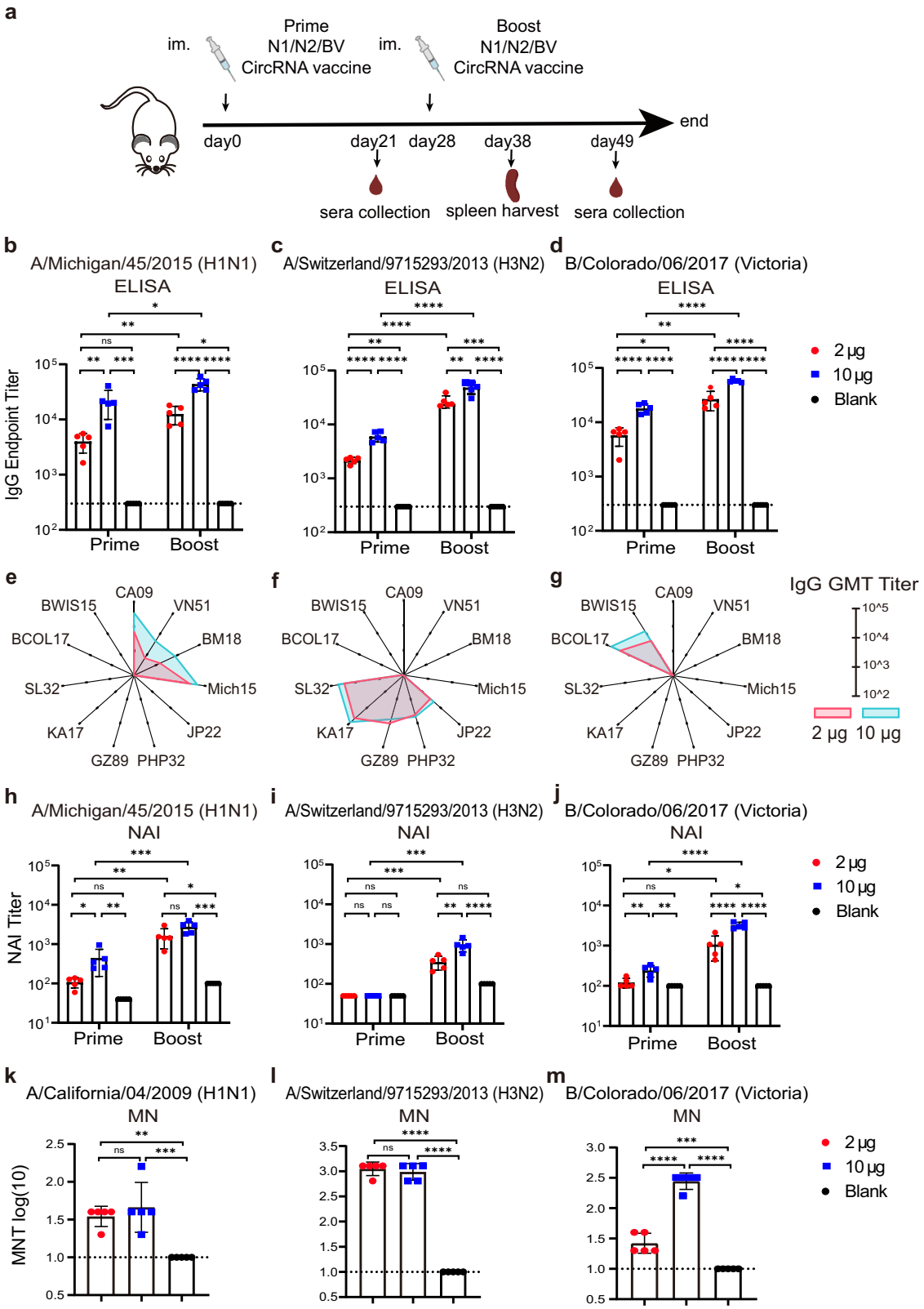

Trivalent circRNA vaccine induced broad-spectrum immunity

Drawing from previous successes in delivering multivalent HA antigens via mRNA LNPs without encountering antigenic competition[36], we developed a trivalent circRNA vaccine. This vaccine combines three distinct circRNA LNPs encoding N1, N2, and IBV antigens. This strategy aims to utilize multivalent antigen delivery to broaden the range of vaccine protection while mitigating antigenic interference. Mice were vaccinated with a combination of N1, N2, and IBV NA circRNA LNPs using two doses: 30 μg (10 μg each NA) and 6 μg (2 μg each NA), with a 4-week boost interval (Fig. 4a).

Sera antibody titers demonstrated that the trivalent circRNA vaccine induced a balanced and robust antibody response against all three NA

Fig. 2 | Monovalent circRNA vaccine induces antibody response in mice. a Five mice per group were immunized with two doses of monovalent circRNA vaccine (N1, N2, IBV) at a four-week interval. Sera were collected 3 weeks after both the prime and boost immunization. A blank LNP group was used as a control. The figure was created by the author using Adobe Illustrator 2020. Binding antibodies against Mich15 (**b**), SL32 (**c**), and BCOL17 (**d**) NA recombinant proteins were detected by ELISA. ELISA was performed to assess the binding ability of N1 monovalent (**e**), N2 monovalent (**f**), IBV monovalent (**g**) circRNA immune sera to heterologous N1, N2, IBV NA recombinant protein. The radar diagram shows the geometric mean titer (GMT) of each group ($n = 5$). The abbreviation of the virus strain was the same as in Fig. S1. NAI antibodies against Mich15 (**h**), SL32 (**i**), and BCOL17 (**j**) were detected by ELLA. Using recombinant protein as antigen. Neutralization titers of boost immune sera against CA09 (**k**), SL32 (**l**), and BCOL17 (**m**) virus were detected by microneutralization assay. Data are presented as the mean ± SD ($n = 5$), and each symbol represents one animal. The dashed lines correspond to the lowest initial dilution. Statistical significance was performed by One-way ANOVA; Unpaired Student's *t* tests were used to compare antibody titers between prime and boost sera within the same dosage group of mice; $^{*}P < 0.05$; $^{**}P < 0.01$; $^{***}P < 0.001$; $^{****}P < 0.0001$; ns, not significant.

components, comparable to monovalent vaccines (Fig. 4b–d). Importantly, there was no significant difference in sera titers between the two dose groups of the trivalent vaccine, possibly due to the saturation of circRNA doses in mice. Notably, trivalent vaccination elicited broader antibody recognition, encompassing all heterologous N1, N2, and IBV strains, exceeding the monovalent response, especially in the high-dose groups (Figs. 2e–g, 4e). Additionally, trivalent sera demonstrated functional neutralization against all three NA subtypes and their respective viruses in vitro (Fig. 4f–k).

Trivalent circRNA vaccine provided broad-spectrum protection in vivo

To assess in vivo protection, mice vaccinated with the trivalent circRNA vaccine were challenged with lethal doses of various influenza strains 28 days after the boost. Against the $5 \times LD_{50}$ of homologous H1N1 strain A/California/04/2009 (CA09), both doses of the trivalent vaccine completely protected all mice, with minimal (~5%) weight loss (Fig. 5a). Even against a more distant H1N1 strain (A/Puerto Rico/8/1934; PR8; 81.8% identity), both doses provided significant protection, although with moderate (~15%) weight loss (Fig. 5b). Similar results were observed for H3N2 strains, with complete protection against the closer A/Gui Zhou/54/1989 (GZ89; 90.4% identity) and the more distant A/Hong Kong/8/1968 (HK68; 85% identity) strains (Fig. 5c, d). The vaccine's role in dampening viral load was further evaluated. At 4 days post-infection (4 dpi), viral load in the lungs of vaccinated mice was significantly lower compared to control groups under the sublethal challenge with CA09 and HK68 strains (Fig. S3a, b).

Similarly, the protective efficacy of the trivalent circRNA vaccine against influenza B virus was also evaluated. Upon the lethal challenge with B/Colorado/06/2017 (BCOL17; homologous to vaccine antigen), mice vaccinated with the trivalent circRNA vaccine were protected from morbidity (Fig. 5e). Lung virus titers were also analyzed at 4 dpi following sublethal challenge with $1 \times LD_{50}$ of B/Malaysia/2506/2004 (BMA04; 96.6% identity) virus. Virus load in the lungs of all mice vaccinated with the trivalent circRNA vaccines was cleared below the detection limit, whereas virus load in the control group reached up to 10^5 PFU (Fig. S3d). The vaccine's protective efficacy against the Yamagata lineage virus B/Florida/4/2006 was evaluated. At 4 dpi, viruses were effectively cleared in mice vaccinated with the trivalent vaccine, particularly in the high-dose group, while viral loads in lung homogenates of control mice exceeded 2×10^5 $TCID_{50}$/ml (Fig. S3c). These findings indicate that the trivalent circRNA vaccine effectively protects mice against diverse strains of H1N1 and H3N2, as well as both Victoria and Yamagata influenza B viruses. These findings highlight the potential value of this platform for developing broad-spectrum influenza vaccines.

One dose of trivalent circRNA vaccines could protect mice

The protective efficacy of the trivalent circRNA vaccine was evaluated in a single-dose vaccination regimen (Fig. 6a). Mice that received a single dose of the trivalent circRNA vaccine at 30 μg and 6 μg doses survived the lethal challenge with B/Colorado/06/2017 (Fig. 6e). These results confirm that trivalent circRNA vaccines effectively protect mice with a single shot.

Discussion

Developing a broad-spectrum influenza vaccine remains a major challenge. Current vaccines primarily target the highly variable HA protein, leading to reduced effectiveness against drifted influenza virus strains. In this study, we designed a circRNA vaccine based on the NA antigen. While NA exhibits less antigenic variation than HA, it is naturally an immune-subdominant antigen. On the surface of the influenza virus, HA is present in greater abundance than NA[37]. This means the immune system often prioritizes HA responses, potentially neglecting conserved NA epitopes. Previous studies successfully induced anti-NA antibodies using enhanced immunization strategies but struggled to target conformational epitopes crucial for neutralization[38]. Since most of the conserved B cell epitopes of NA depend on natural conformation, inducing antibodies towards these conformational epitopes remained a significant challenge.

To address this challenge, we utilized circRNA technology to deliver membrane-bound NA as the immunogen. Antigens encoded by circRNA mimic the natural conformation in the natural infection, thereby preserving key epitopes. Considering the safety of the vaccine, we chose a clinically validated LNP formulation. In our study, SM102-based LNPs were effective in delivering circRNA, and the safety profile is crucial for facilitating future clinical translation of the vaccine. A similar strategy has proven successful in mRNA vaccines, incorporating components such as HA stalk, NA, matrix-2 ion channel, and nucleoprotein in multivalent mRNA vaccines that induced protective effects against multi-strain influenza viruses[20]. Compared to mRNA, circRNA offer increased cellular stability due to their closed-loop structure[24]. This extended antigen presence could enhance B cell maturation and production of high affinity antibodies. These results confirm robust NA-specific antibody responses in mice receiving monovalent and trivalent circRNA vaccines (Figs. 2, 4).

Following booster immunization in this study, the vaccine induced a robust NA-reactive antibody response, as evidenced by high NAI antibody titers exceeding 1000 (Fig. 4f–h). These results suggest that boost immunization may be necessary to generate sufficient antibodies against enzyme-active sites. Unlike mice with a naive immune background, the population has preexisting low levels of NA-reactive antibodies[39]. This suggests the potential of utilizing this immune memory to enhance a robust immune response through an appropriate vaccination strategy. Future experiments should systematically evaluate how circRNA vaccines induce immune responses in mice previously exposed to influenza. A single dose of circRNA vaccine has the potential to reactivate NA-specific immune memory, but further experimental validation of this hypothesis is crucial.

CircRNA vaccine induced NAI antibodies against BCOL17, which is genetically closely related to the vaccine strain (Fig. S1) and can inhibit virus replication in vitro and in vivo. Although cross-reactive antibodies within the same subtype were induced, no cross-reactive between subtypes was observed, consistent with previous findings on NA-specific responses[40]. This highlights the ongoing challenge of eliciting broad-spectrum immunity against heterologous NA strains. Future strategies may involve incorporating more NA subtypes or designing immunogens focused on highly conserved enzyme active sites.

NA vaccines can still confer protection even when neutralization is limited[20]. Beyond humoral immunity, this study also revealed a robust T cell response induced by the circRNA vaccines. However, the $CD8^+$ T cell response to SL32 N2 was less robust than that of N1 and BV (Fig. 3f). IFN-γ levels were higher than IL-4, indicating a Th1-biased immune response (Fig. 3a–e). This is further supported by the increased IgG2a: IgG1 ratio in vaccinated mice (Fig. S4). Th1-biased response with higher IgG2a level was

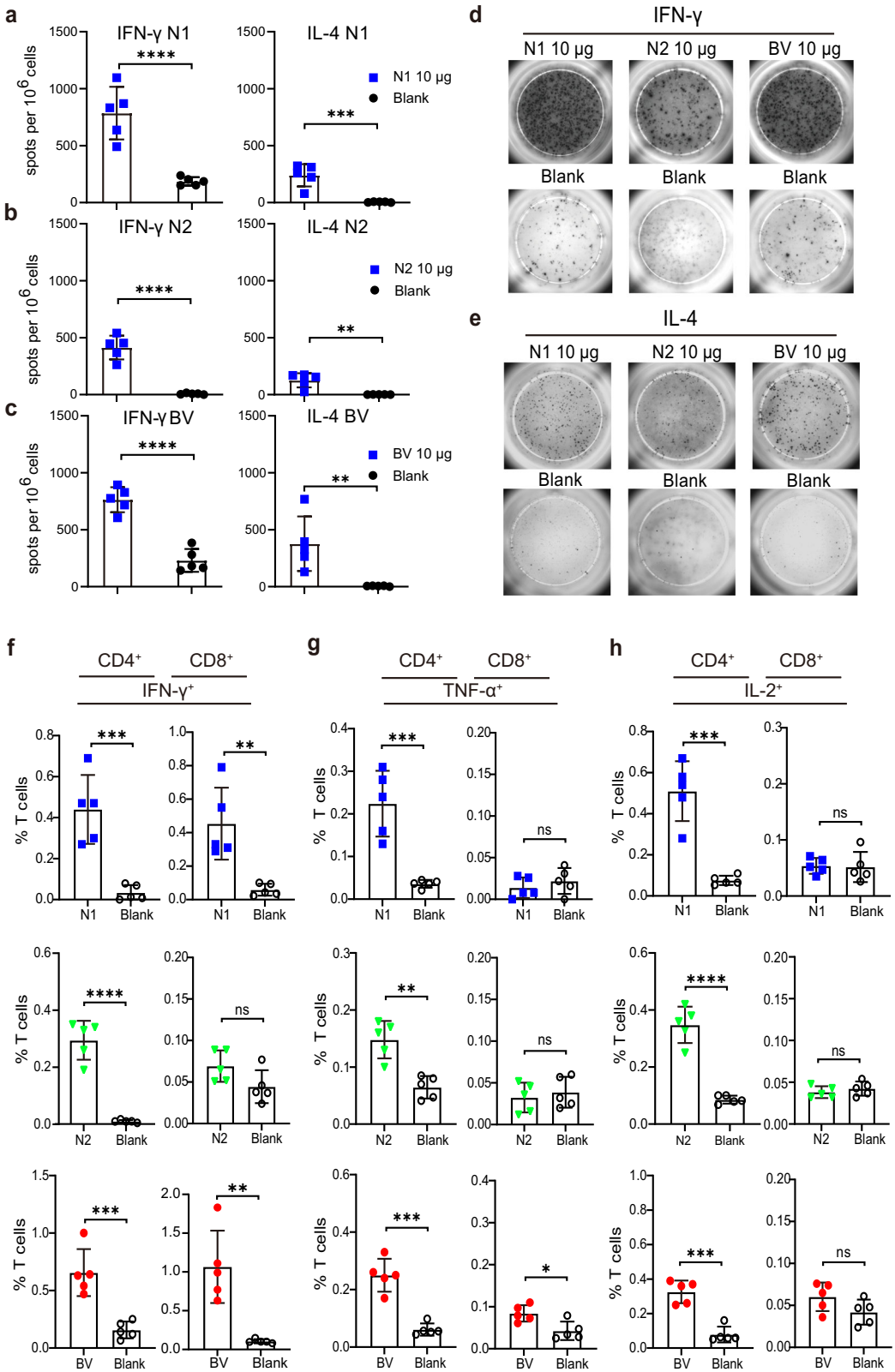

Fig. 3 | CircRNA vaccination induced NA-specific cellular responses. a–c Mice were vaccinated with 10 μg of circRNA-LNP encoding N1, N2, or IBV NA, following a prime-boost vaccination scheme. Ten days post boost vaccination, the spleen was harvested and spot-counting for IFN-γ/IL-4 -secreting cells by ELISpot assay after stimulating with N1 (**a**), N2 (**b**) or IBV NA (**c**) recombinant protein. Representative walls of IFN-γ (**d**) or IL-4 (**e**) ELISpot. The proportion of IFN-γ (**f**), TNF-α (**g**), or IL-2 (**h**) secreting $CD4^+$ and $CD8^+$ T cells was assessed by FASC. Splenocytes from the blank LNP group were used as a control. Data are presented as the mean ± SD ($n = 5$), and each symbol represents one animal. Statistical significance was performed by unpaired t test; $^*P < 0.05$; $^{**}P < 0.01$; $^{***}P < 0.001$; $^{****}P < 0.0001$; ns, not significant.

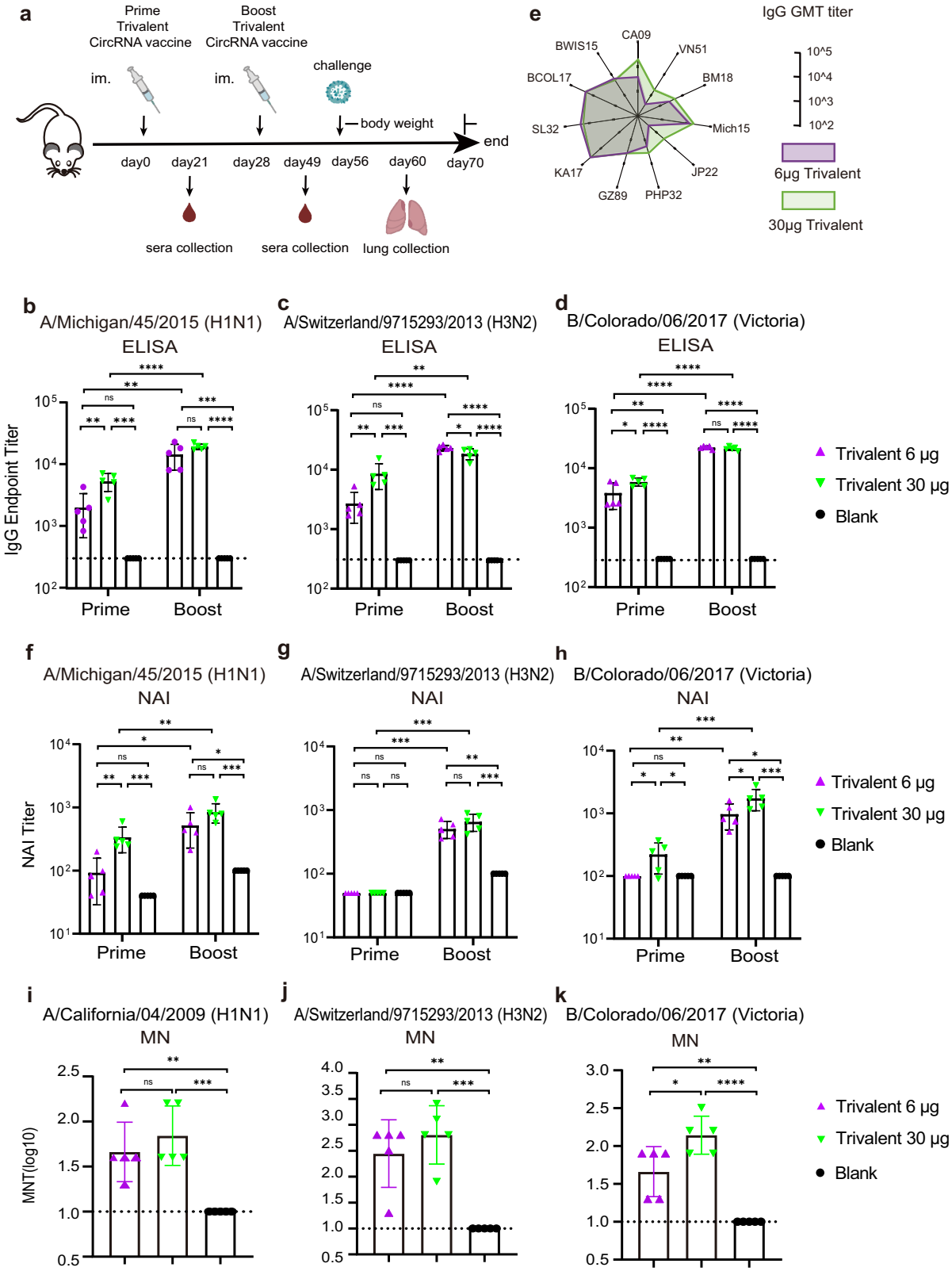

known to be beneficial for clearing virus infections and reducing the risk of vaccine-associated enhanced respiratory disease (VAERD)[41–44]. While the role of NA-specific T cells has been relatively underexplored in previous studies, recent research on mRNA vaccines has highlighted their potential importance[20]. Similar cross-protection against heterologous strains such as GZ89, PR8, and HK68 was observed in this study. Although the trivalent circRNA vaccine sera did not neutralize these strains (Fig. S5), vaccinated mice exhibited complete survival upon challenge. Furthermore, Fc-mediated effector responses, such as ADCC, antibody-dependent cellular phagocytosis (ADCP), and complement-dependent cytotoxicity (CDC), may also contribute to vaccine protection[45,46]. The limitation of this study was the need to characterize these effects further. NA, as a membrane

Fig. 4 | Trivalent circRNA vaccine induced a balanced immune response against N1, N2, and influenza B NA. a Trivalent circRNA vaccine immunization and challenge regimen. Mice received a prime-boost immunization program with 4 weeks intervals, 4 weeks after boost vaccination mice were challenged with $5 \times LD_{50}$ or $1 \times LD_{50}$ influenza virus. Body weight and survival rate were monitored for 14 days. Some mice were euthanized, and lungs were collected at 4 dpi. A blank LNP group was used as a control. The figure was created by the author using Adobe Illustrator 2020. ELISA was used to measure the binding antibody titers against Mich15 (**b**), SL32 (**c**), and BCOL17 (**d**) in the serum samples from the trivalent vaccine group. **e** The binding breadth of trivalent vaccine immune sera after boost vaccination. The radar diagram shows each group's geometric mean titer (GMT) ($n = 5$). The abbreviation of the virus strain was the same as in Fig. S1. NAI titer of trivalent immune sera. NA inhibition antibody titers against Mich15 (**f**), SL32 (**g**), and BCOL17 (**h**) were detected by ELLA. Neutralization titer of boost immune sera for trivalent vaccine. Microneutralization titers against CA09 (**i**), SL32 (**j**), and BCOL17 (**k**) virus were detected by microneutralization assay. Data are presented as the mean ± SD ($n = 5$), and each symbol represents one animal. The dashed lines correspond to the lowest initial dilution. Statistical significance was performed by One-way ANOVA; Unpaired Student's t tests were used to compare antibody titers between prime and boost sera within the same dosage group of mice; $^{*}P < 0.05$; $^{**}P < 0.01$; $^{***}P < 0.001$; $^{****}P < 0.0001$. ns, not significant.

protein, simultaneously stimulates T cell response, NAI antibodies, and Fc-mediated effector functions such as ADCC, CDC, and ADCP are likely to play a more comprehensive protective role, offering broad protection against a wide range of strains.

The trivalent vaccines provided protection to mice with a single dose (Fig. 6). Given that a multi-dose immunization process may decrease public acceptance, this suggests that a prime-only approach can serve as an alternative vaccination regimen. Furthermore, the vaccine exhibited protection against Yamagata lineage viruses even in the absence of specific Yamagata lineage antigens (Fig. S3c). Sequence analyses between the vaccine's N2 antigen and prevalent N2 strains suggest that the trivalent circRNA vaccine could be effective against contemporary H3N2 strains due to their closer antigenic resemblance compared to the GZ89 and HK68 strains (Fig. S6). These findings highlight the potential of this vaccine as a promising candidate for the seasonal influenza vaccines.

In conclusion, this study demonstrates the feasibility of delivering combined NA immunogens through circRNA technology to achieve broad-spectrum protection. The trivalent circRNA vaccine effectively protected mice against diverse H1N1, H3N2, and influenza B viruses. This protection likely involves a combination of NAI, Fc-mediated effector functions, and NA-specific T cell responses. These findings reinforce the potential of circRNA as a promising platform for influenza vaccines and highlight the importance of NA in developing universal vaccines. By building upon this work, circRNA can demonstrate its potential as a platform for broad-spectrum vaccines.

Methods

Cells

The human embryonic kidney (HEK) 293 T cells, *Spodoptera frugiperda* (Sf9) insect cells, and Madin Darby Canine Kidney (MDCK) cells were purchased from the American Type Culture Collection (ATCC). The HEK293T and MDCK cells were cultured in Dulbecco's Modified Eagle's Medium (DMEM, Gibco, U.S.) supplemented with 10% fetal bovine serum (FBS, Gibco, U.S.) and 1% penicillin-streptomycin solution (Gibco, U.S.) at 37 °C with 5% CO_2. The Sf9 cells were cultured in SF-SFM medium (Suzhou world-medium Biotechnology Co., Ltd., Suzhou, China) supplemented with 1% penicillin-streptomycin solution (Gibco, U.S.), at 27 °C in the dark, using a cell shaker setting at 110 rpm.

Virus and recombinant NA protein

All influenza viruses were grown in 10-day-old specific-pathogen-free (SPF) embryonated chicken eggs. Influenza A virus was cultured at 37 °C for 48 h, while influenza B virus was cultured at 33 °C for 72 h. Then the eggs were chilled at 4 °C overnight. The next day, the allantoic fluid was harvested, filtered, and centrifuged at the speed of $10,000 \times g$ at 4 °C for 10 min. Finally, the virus was stored at −80 °C. Virus titer was determined by $TCID_{50}$ assay. To prepare the virus for the challenge experiment, the collected allantoic fluid was ultracentrifuged on an Optima XPN-100 ultracentrifuge (Beckman, U.S.) at the speed of $130,000 \times g$ at 4 °C for 2 h to precipitate the virus. The virus pellet was resuspended in 1 × phosphate-buffered saline (PBS) and further purified by passing through a 30% sucrose cushion. The purified virus was aliquoted and stored at −80 °C.

All recombinant NAs were expressed in the Sf9 cells, as described in the previous study[47]. Recombinant NAs were purified by Ni^{+} Sepharose high-performance chromatography.

CircRNA design and synthesis

CircRNA was generated using the PIE splicing strategy[23]. Linear precursor RNAs were transcribed from linearized plasmid templates using T7 RNA polymerase (Thermo, U.S.). After treatment with DNase I (New England Biolabs, USA), RNAs were purified using an RNA purification kit (Magen Biotechnology Co., Ltd., Guangzhou, China). For the RNA cyclization reaction, purified RNA was first heated to 70 °C for 5 min and immediately placed on ice. The reaction solution was added, containing a final concentration of 2 mM Guanosine triphosphate (GTP), 50 mM Tris-HCl (pH 7.5), 10 mM $MgCl_2$, and 1 mM DTT. The RNA cyclization reaction was performed at 55 °C for 8 min, then RNase R (New England Biolabs, USA) was added to the reaction and incubated at 37 °C for 15 min to remove uncirculated RNA. CircRNA was finally column purified using the RNA purification kit (Magen Biotechnology Co., Ltd., Guangzhou, China) and stored at −80 °C. According to the previous study[23], the quality and integrity of circRNAs were assessed by 1.5% agarose gel electrophoresis at 160 V for 30 min.

LNP encapsulated circRNA

LNPs were generated by rapidly mixing the organic and aqueous phases (1:3, v/v) through the iNanoE microfluidic system (Micro & Nano (Shanghai) Biologics Co. Ltd., Shanghai, China) at a total flow rate of 12 mL/min. The organic phase was formed by mixing SM102, 1,2-Distearoyl-sn-glycero-3-phosphorylcholine (DSPC), cholesterol, and DMG-PEG2000 (AVT (Shanghai) Pharmaceutical Tech Co., Ltd) in ethanol with a molar ratio of 50:10:38.5:1.5. The circRNA was dissolved in 50 mM citric acid buffer (pH = 4). The N/P ratio of ionizable lipids and circRNA was 4:1. The formed LNPs were diluted 40-fold in PBS and concentrated using a 100 kDa ultrafiltration tube (Millipore, U.S.). The encapsulation efficiency of LNP was determined following the method described previously[48]. To characterize particle size and PDI, LNPs were added to the cuvette after 40-fold dilution by PBS, and dynamic light scattering (DLS) was performed using Zetasizer Pro (Malvern Panalytical, England), with three replicates of measurements for each sample, and PBS as a negative sample control.

CircRNA-LNP transfection and flow cytometric analyses

Before transfection, HEK293T cells were seeded in 24-well plates at a density of 6×10^5. The following day, 500 ng of each LNP encapsulated circRNA was diluted in DMEM and added to cells. After 48 h, the cells were harvested and washed with 1% Bovine Serum Albumin (BSA) Fraction V in 1 × PBS. Then cells were incubated with 10 μg/mL anti-NA antibodies: 1G01, 229-2C06, or CC61 for 20 min on ice. After that, cells were washed twice with 1% BSA PBS and incubated with 1: 2000 dilution of rabbit anti-human IgG(H + L) FITC (Southern Biotech, U.S.) for 20 min on ice in the dark. Cells were washed twice and resuspended. Flow cytometric data were acquired on CytoFLEX S flow cytometer (Beckman, U.S.). Approximately 50,000 events were collected per sample.

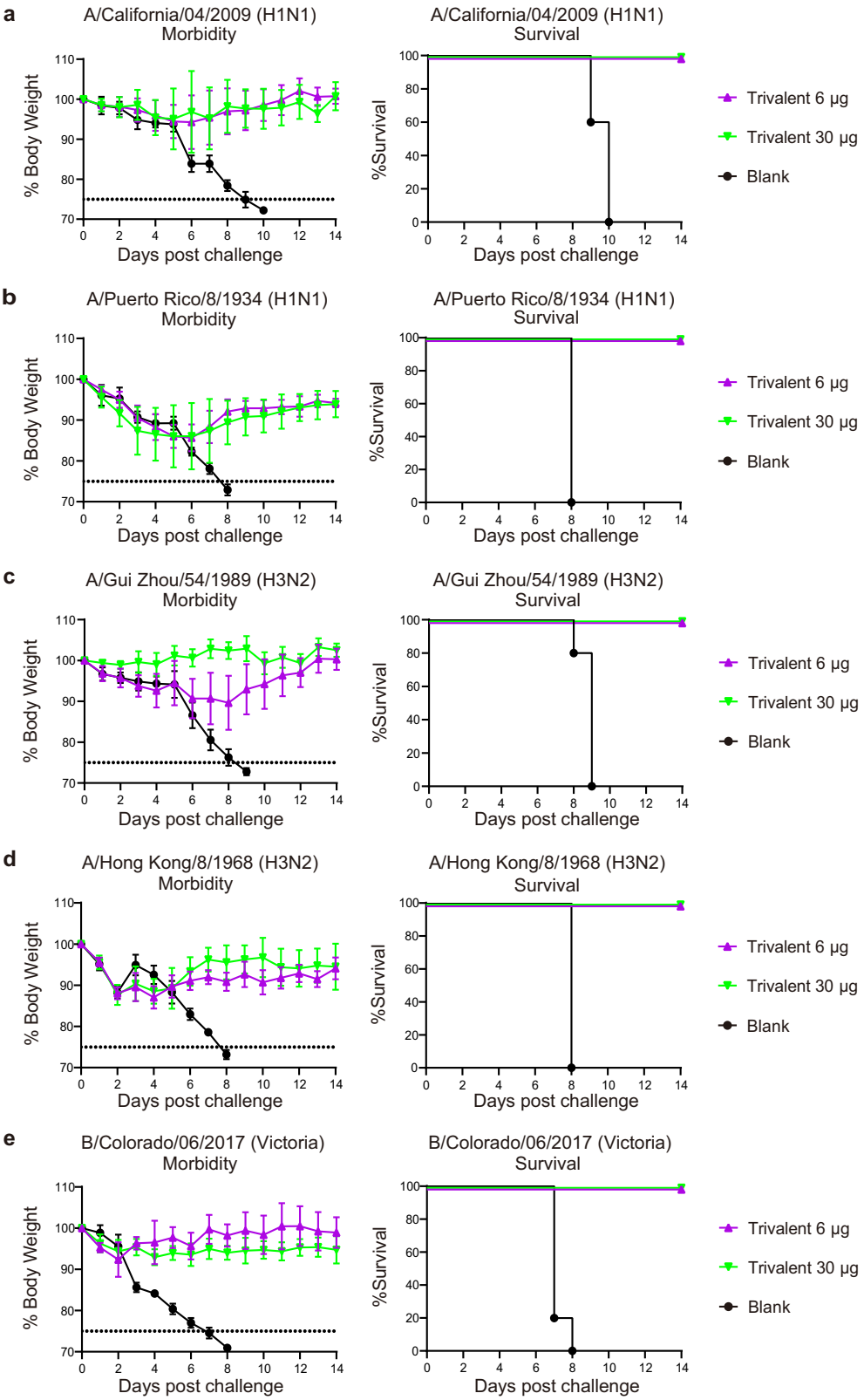

Fig. 5 | Trivalent circRNA vaccine protects mice from heterologous virus challenge. a–e Mice ($n = 5$) were immunized with 6 μg or 30 μg trivalent CircRNA vaccine in two doses at 28-day intervals. Blank LNP was used as a control. Twenty-eight days post boost vaccination, mice were challenged $5 \times LD_{50}$ of A/California/04/2009(H1N1) (**a**), A/Puerto Rico/8/1934 (H1N1) (**b**), A/Gui Zhou/54/89 (H3N2) (**c**), A/Hong Kong/8/1968 (H3N2) (**d**), B/Colorado/06/2017(Victoria) (**e**). Body weight and survival rate were monitored for 14 days. Body weight was shown as the mean of five mice ± SD.

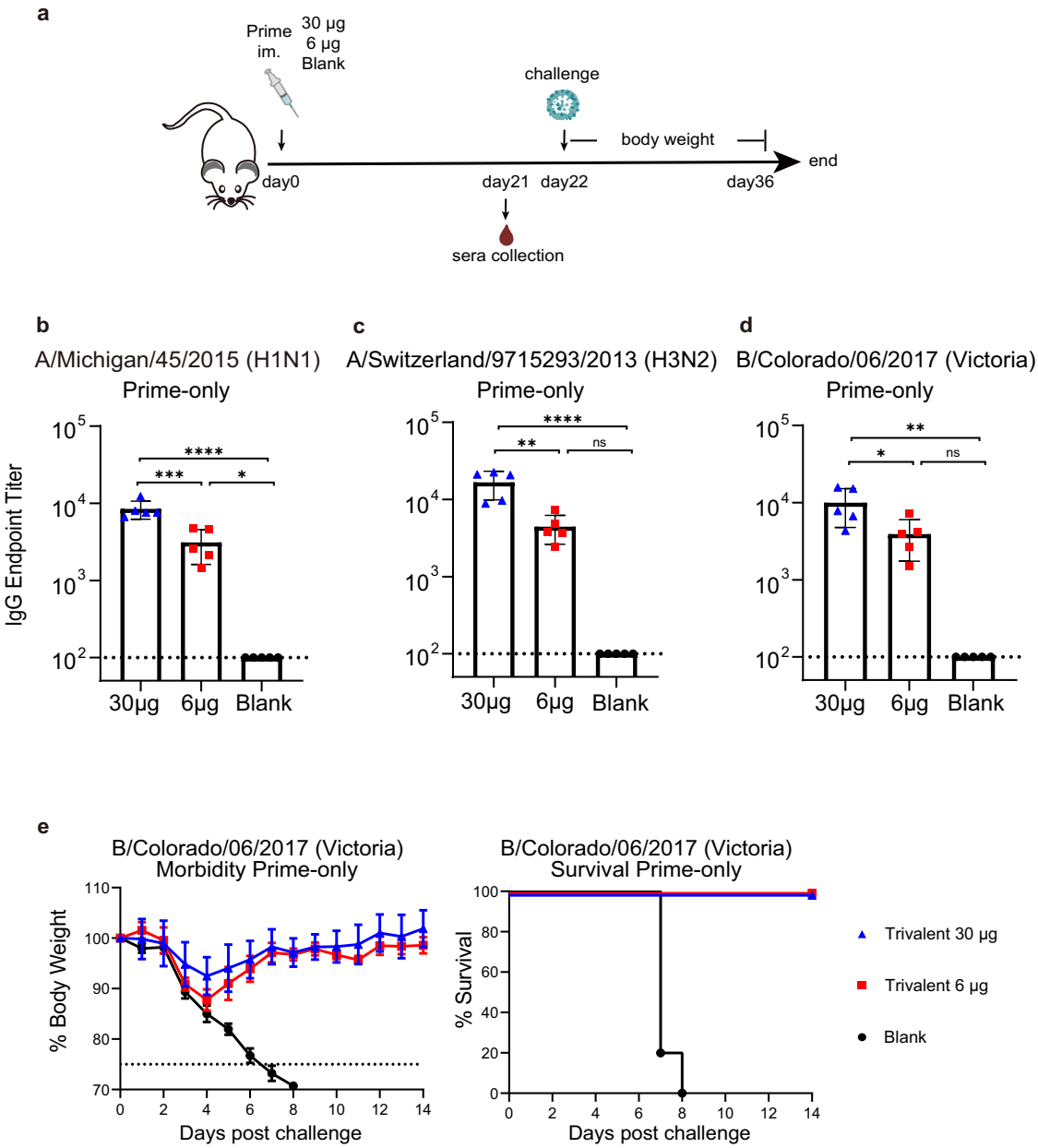

Fig. 6 | Protective efficacy of a single dose of circRNA vaccine. a Immunization schedule for the challenge experiment in the prime-only group. The figure was created by the author using Adobe Illustrator 2020. **b–d** Antibody titers against the NA recombinant proteins from Mich15 (**c**), SL32 (**d**), and BCOL17 (**e**) were measured using ELISA. The data present results from five mice per group. Dashed lines indicate the lowest initial dilution. Statistical significance was determined using One-way ANOVA; $^{*}P < 0.05$; $^{**}P < 0.01$; $^{***}P < 0.001$; $^{****}P < 0.0001$; ns denotes not significant. **e** Mice ($n = 5$) in the prime-only group were challenged with $5 \times LD_{50}$ of B/Colorado/06/2017 (Victoria) virus. Body weight and survival rate were monitored for 14 days. Body weight was shown as the mean of five mice ± SD.

MUNANA assay

LNP transfected cells were diluted at the density 1×10^6 in MUNANA buffer (33.3 mM MES, 4 mM $CaCl_2$, pH 6.5). The cells were two-fold serially diluted using MUNANA buffer in a black 96-well plate to make a 50 μL final volume. Then, 50 μL of 300 μM of MUNANA substrate was added. After incubating at 37 °C for 1 h, 100 μL of stop solution (138.6 mM NaOH in absolute ethanol) was added. The plate was read using a SYNERGY H1 (BioTek, US) multimode microplate reader with 355 nm excitation and 460 nm emission.

Vaccination and virus challenge

6–8-week-old female BALB/c mice ($n = 5$ per group) were intramuscularly injected with 100 μL circRNA vaccine diluted in PBS. Trivalent circRNA vaccines were formulated with equal amounts of three NA circRNA vaccines. Boost vaccination was performed 28 days after prime vaccination. Twenty-eight days after boost vaccination, mice were anesthetized with avertin (250 mg/kg) and intranasally infected with $5 \times LD_{50}$ influenza virus in 30 μL PBS. The body weight was monitored for 14 days after infections, and mice that lost over 25% of their initial weight were humanely euthanized. The weighing order was randomly assigned each day, and each group of mice was weighed in a different order each day. The animals were grouped and manipulated by different individuals. The experimental operators were unaware of the specific grouping. All mice were kept in a SPF environment, and all virus challenge experiments were performed in an animal biosafety level 2 laboratory.

For the euthanasia of mice, animals were initially anesthetized with Avertin (250 mg/kg) via intraperitoneal injection. Subsequently, euthanasia was carried out by cervical dislocation after confirming their lack of

responsiveness to pain and stimuli (deep anesthesia). Euthanasia was carried out following the American Veterinary Medical Association (AVMA) Guidelines.

ELISA

The 96-well ELISA plates were coated with recombinant NA proteins (50 μL, 200 ng/well) or trivalent inactivated vaccine (TIV, Southern hemisphere, 2022-2023) in PBS at 4 °C overnight. The following day, the plates were blocked with 150 μL 3% BSA at 37 °C for 1 h. The sera were serially diluted 3-fold, starting with a 1:300 dilution (or 1:100 in the prime group for Fig. 6), and then added to the plates. The plates were subsequently incubated at 37 °C for 1 h. Following washing with PBST (PBS added with 0.05% TWEEN 20), 75 μL of 1: 4000 dilution of HRP-conjugated anti-mouse IgG/IgG1/IgG2a secondary antibody (Southern Biotech, U.S.) was added to plates and incubated at 37 °C for 1 h. The readout was developed using 2,2'-Azino-bis (3-Ethylbenzthiazoline-6-Sulfonic Acid, ABTS) ELISA substrate (sigma, U.S.). After 20 min of incubation, absorbance was measured at 405 nm on a Spectramax ABS Plus (Molecular Devices, U.S.) microplate reader. Endpoint titers were defined as the dilution fold with OD value exceeding 2 × background (without sera, but the secondary antibody was added). Monoclonal antibody 1G01[10] was used as positive control.

Enzyme-linked lectin assay (ELLA)

The 96-well ELISA plates were pre-coated with 100 μL of fetuin (Sigma, U.S.) at 25 μg/mL in PBS and incubated at 4 °C for 24 h, then the plates were washed three times with PBST. Heat-inactivated sera were 2-fold serially diluted starting with a 1:50 dilution (in some groups were 1:100) in DPBS-T-BSA buffer (Dulbecco's phosphate-buffered saline containing 0.133 g/L $CaCl_2$ and 0.1 g/L $MgCl_2$ with 0.05% Tween-20 and 1% BSA) and mixed with an equal volume of virus or NA recombinant proteins. The mixtures were incubated at 37 °C for 2 h and then transferred to the fetuin-coated plates. The plates were incubated at 37 °C for 18 h and washed six times with PBST subsequently. Then 100 μL/well of HRP-conjugated peanut agglutinin lectin (Sigma, U.S.) in PBS was added to the plates and left in the dark for 2 h at room temperature. After adding the ABTS ELISA substrate and 15 min of incubation, the absorbance of the samples was read at 405 nm on a Spectramax ABS Plus (Molecular Devices, U.S.) microplate reader. The samples that did not reach 50% inhibition at the initial sera dilution were considered negative.

Microneutralization assay

For the microneutralization assay, sera were treated with the receptor-destroying enzyme (RDE, Denka Seiken, Japan) and then inactivated at 56 °C for 30 min. Sera were then diluted 2-fold serially starting at 1:10 dilutions in infection media (DMEM supplemented with 1 μg/mL TPCK-treated trypsin, 0.1 mM MEM non-essential amino acid, 1% penicillin-streptomycin solution). Next, 60 μL of diluted sera were mixed with 60 μL of 100 × $TCID_{50}$ virus and incubated at 37 °C for 1 h. Then the virus-sera mixtures were transferred to the PBS-washed MDCK cells and incubated at 37 °C with 5% CO_2 for 1 h. After washing with PBS twice, 100 μL of infection medium with the same sera dilution was added to the cells. Following incubation at 37 °C for 48 h (for influenza A virus) or 33 °C for 72 h (for influenza B virus). Virus replication was detected using a hemagglutination assay. Briefly, 50 μL of cell supernatant was transferred into a 96-well V-bottom plate, followed by the addition of 25 μL of 1% chicken red blood cells (RBCs). After incubating at room temperature for 15 mins, the presence of virus was determined by observing hemagglutination of the RBCs. The neutralization titer of sera was determined as the highest dilution at which no virus was detected.

ELISPOT assay

The day before assay, 1:100 anti-mouse IFN-γ or IL-4 antibody (U-Cytech, Netherland) was added to ELISpot plate (Millipore, U.S.) and incubated at 4 °C overnight. The Next day, plates were blocked with 10% FBS in RPMI 1640 medium at 37 °C for 1 h. Next 4×10^5 Splenocytes were added to the ELISPOT plate and stimulated by 10 μg/mL recombinant NA protein at 37 °C in 5% CO_2 for 40 h. The plates were washed with PBST 6 times and incubated with 1:100 biotinylated antibody for 2 h at RT. After washing, the plates were incubated with 1:500 Streptavidin-HRP for 1 h at RT. Finally, the plates were incubated with 5-bromo-4chloro-3-indolyl-phosphate/nitro blue tetrazolium (BCIP/NBT, Beyotime, China) substrate solution for 5 min, and scanned using Mabtech IRIS FluoroSpot/ELISpot reader (Mabtech, Sweden).

Intracellular cytokine staining assay

The splenocytes were isolated and plated at a density of 4×10^6 per well in a round-bottom 96-well plate and stimulated with 10 μg/mL recombinant NA protein at 37 °C, 5% CO_2 for 6 h. Brefeldin A was then added to each sample and cells were incubated for an additional 4 h. After incubation, cells were washed with PBS and stained with LIVE/DEAD cell staining solution (Biolegend, U.S.) for 30 min in the dark. After washing with FASC buffer (PBS added 2% FBS), cells were then incubated with Fc Blocker (Biolegend, #101319, U.S.) for 5 min in dark and then surface-stained with the following antibodies: anti-CD3-Pacific Blue™ (Biolegend, #100214, U.S.); anti-CD4-FITC (Biolegend, #100509, U.S.); anti-CD8α-Brilliant Violet 605 (Biolegend, #100744, U.S.). After fixation with a fixation/permeabilization solution (Beyotime, China), cells were intracellularly stained with the following antibodies: anti-IFN-γ-APC (Biolegend, #505810, U.S.); anti-TNF-α-Brilliant Violet 785™ (Biolegend, #506341, U.S.); anti-IL-2-PE-Cyanine7 (Biolegend, #503832, U.S.) for 30 min in dark. Finally, cells were washed twice using permeabilization buffer and suspended in FASC buffer. Flow cytometric analysis and cell sorting were performed on CytoFLEX S Flow Cytometer (Beckman Coulter, U.S.). Analysis was performed using FlowJo software V_10.

Virus plaque assay and $TCID_{50}$ assay

Mice were sacrificed and lungs were homogenized in 10% (w/v) DMEM at 4 dpi. The lung homogenate was diluted in a 1:10 series and inoculated into a 6-well plate containing a single layer of MDCK cells. After 1 h of incubation, the plates were washed twice with PBS and 2 mL overlay (2 × DMEM, 1 μg/mL TPCK-treated trypsin, 0.1 mM MEM non-essential amino acid, 1% penicillin-streptomycin solution, 0.8% low melting agar) was added. After 72 h of culture, the agar overlays were removed, and the cells were fixed and stained with a crystal violet solution.

To determine the $TCID_{50}$, the lung homogenate was 3-fold serially diluted in DMEM starting at 1:10. MDCK monolayers in 96-well plates were washed twice with PBS before adding 100 μL of the diluted lung homogenate. After incubating at 37 °C with 5% CO_2 for 1 h, cells were washed with PBS, followed by adding 100 μL of infection media. Influenza A virus-infected cells were further cultured at 37 °C with 5% CO_2 for 48 h, while influenza B virus-infected cells were incubated at 33 °C with 5% CO_2 for 72 h. Hemagglutination assay was performed as described in 10. $TCID_{50}$ was calculated using the Reed-Muench method.

Phylogenetic tree analysis

All NA sequences involved in this study were downloaded from the NCBI database (https://www.ncbi.nlm.nih.gov/). NA phylogenetic tree was generated by MAGAX using the Maximum Likelihood method.

Statistical analysis

Statistical analyses were performed using the Prism 9.0 software (GraphPad, U.S.). All errors are expressed as means with standard derivation (±SD). In Figs. 2 and 4, one-way ANOVA with multiple comparison tests was employed to compare antibody titers among different groups within the prime or boost immunization phases. Unpaired Student's *t* tests were used to compare antibody titers between prime and boost sera within the same dosage group of mice. Unpaired Student's *t* test analysis was performed to determine *p* values in T cell responses. Group data were considered statistically significant when $p < 0.05$, and*, **, ***, ****, and ns in results represent $p < 0.05$, $p < 0.01$, $p < 0.001$, $p < 0.0001$, and not significant, respectively.

Data availability

The authors declare that the data are publicly available or will be available upon request

Received: 6 April 2024; Accepted: 1 September 2024;
Published online: 16 September 2024

References

1. Wu, N. C. & Ellebedy, A. H. Targeting neuraminidase: the next frontier for broadly protective influenza vaccines. *Trends Immunol.* **45**, 11–19 (2024).
2. Krammer, F. et al. NAction! How can neuraminidase-based immunity contribute to better influenza virus vaccines? *mBio* **9**, e0233217 (2018).
3. Zhang, X. & Ross, T. M. Anti-neuraminidase immunity in the combat against influenza. *Expert Rev. Vaccines* **23**, 474–484 (2024).
4. Giurgea, L. T., Morens, D. M., Taubenberger, J. K. & Memoli, M. J. Influenza neuraminidase: a neglected protein and its potential for a better influenza vaccine. *Vaccines* **8**, https://doi.org/10.3390/vaccines8030409 (2020).
5. Chen, Y. Q. et al. Influenza infection in humans induces broadly cross-reactive and protective neuraminidase-reactive antibodies. *Cell* **173**, 417–429.e410 (2018).
6. Momont, C. et al. A pan-influenza antibody inhibiting neuraminidase via receptor mimicry. *Nature* **618**, 590–597 (2023).
7. Hansen, L. et al. Human anti-N1 monoclonal antibodies elicited by pandemic H1N1 virus infection broadly inhibit HxN1 viruses in vitro and in vivo. *Immunity* **56**, 1927–1938.e1928 (2023).
8. Lei, R. et al. Leveraging vaccination-induced protective antibodies to define conserved epitopes on influenza N2 neuraminidase. *Immunity* **56**, 2621–2634.e2626 (2023).
9. Lederhofer, J. et al. Protective human monoclonal antibodies target conserved sites of vulnerability on the underside of influenza virus neuraminidase. *Immunity*, https://doi.org/10.1016/j.immuni.2024.02.003 (2024).
10. Stadlbauer, D. et al. Broadly protective human antibodies that target the active site of influenza virus neuraminidase. *Science* **366**, 499–504 (2019).
11. Tan, J. et al. Human anti-neuraminidase antibodies reduce airborne transmission of clinical influenza virus isolates in the Guinea Pig Model. *J. Virol.* **96**, e0142121 (2022).
12. McMahon, M. et al. Immunity induced by vaccination with recombinant influenza B virus neuraminidase protein breaks viral transmission chains in guinea pigs in an exposure intensity-dependent manner. *J. Virol.* **97**, e0105723 (2023).
13. Memoli, M. J. et al. Evaluation of antihemagglutinin and antineuraminidase antibodies as correlates of protection in an influenza A/H1N1 virus healthy human challenge model. *mBio* **7**, e00417–00416 (2016).
14. Strohmeier, S. et al. A CpG 1018 adjuvanted neuraminidase vaccine provides robust protection from influenza virus challenge in mice. *NPJ Vaccines* **7**, 81 (2022).
15. Johansson, B. E., Matthews, J. T. & Kilbourne, E. D. Supplementation of conventional influenza A vaccine with purified viral neuraminidase results in a balanced and broadened immune response. *Vaccine* **16**, 1009–1015 (1998).
16. Strohmeier, S. et al. A novel recombinant influenza virus neuraminidase vaccine candidate stabilized by a measles virus phosphoprotein tetramerization domain provides robust protection from virus challenge in the mouse model. *mBio* **12**, e0224121 (2021).
17. Gao, J. et al. Balancing the influenza neuraminidase and hemagglutinin responses by exchanging the vaccine virus backbone. *PLoS Pathog.* **17**, e1009171 (2021).
18. Broecker, F. et al. Extending the stalk enhances immunogenicity of the influenza virus neuraminidase. *J. Virol.* **93**, 10–1128 (2019).
19. Chivukula, S. et al. Development of multivalent mRNA vaccine candidates for seasonal or pandemic influenza. *NPJ Vaccines* **6**, 153 (2021).
20. Freyn, A. W. et al. A multi-targeting, nucleoside-modified mRNA influenza virus vaccine provides broad protection in mice. *Mol. Ther.* **28**, 1569–1584 (2020).
21. McMahon, M. et al. Assessment of a quadrivalent nucleoside-modified mRNA vaccine that protects against group 2 influenza viruses. *Proc. Natl. Acad. Sci. USA* **119**, e2206333119 (2022).
22. Pardi, N. et al. Development of a pentavalent broadly protective nucleoside-modified mRNA vaccine against influenza B viruses. *Nat. Commun.* **13**, 4677 (2022).
23. Wesselhoeft, R. A., Kowalski, P. S. & Anderson, D. G. Engineering circular RNA for potent and stable translation in eukaryotic cells. *Nat. Commun.* **9**, 2629 (2018).
24. Qu, L. et al. Circular RNA vaccines against SARS-CoV-2 and emerging variants. *Cell* **185**, 1728–1744.e1716 (2022).
25. Amaya, L. et al. Circular RNA vaccine induces potent T cell responses. *Proc. Natl. Acad. Sci. USA* **120**, e2302191120 (2023).
26. Jansen, J. M., Gerlach, T., Elbahesh, H., Rimmelzwaan, G. F. & Saletti, G. Influenza virus-specific CD4+ and CD8+ T cell-mediated immunity induced by infection and vaccination. *J. Clin. Virol.* **119**, 44–52 (2019).
27. Koutsakos, M. et al. Human CD8+ T cell cross-reactivity across influenza A, B and C viruses. *Nat. Immunol.* **20**, 613–625 (2019).
28. van de Ven, K. et al. A universal influenza mRNA vaccine candidate boosts T cell responses and reduces zoonotic influenza virus disease in ferrets. *Sci. Adv.* **8**, eadc9937 (2022).
29. Koutsakos, M., Wheatley, A. K., Laurie, K., Kent, S. J. & Rockman, S. Influenza lineage extinction during the COVID-19 pandemic? *Nat. Rev. Microbiol.* **19**, 741–742 (2021).
30. Sultana, I. et al. Stability of neuraminidase in inactivated influenza vaccines. *Vaccine* **32**, 2225–2230 (2014).
31. Weiss, C. D. et al. Neutralizing and neuraminidase antibodies correlate with protection against influenza during a late season A/H3N2 outbreak among unvaccinated military recruits. *Clin. Infect. Dis.* **71**, 3096–3102 (2020).
32. Couch, R. B. et al. Antibody correlates and predictors of immunity to naturally occurring influenza in humans and the importance of antibody to the neuraminidase. *J. Infect. Dis.* **207**, 974–981 (2013).
33. Corbett, K. S. et al. SARS-CoV-2 mRNA vaccine design enabled by prototype pathogen preparedness. *Nature* **586**, 567–571 (2020).
34. Vogel, A. B. et al. BNT162b vaccines protect rhesus macaques from SARS-CoV-2. *Nature* **592**, 283–289 (2021).
35. Zhang, N. N. et al. A Thermostable mRNA Vaccine against COVID-19. *cell* **182**, 1271–1283.e1216 (2020).
36. Arevalo, C. P. et al. A multivalent nucleoside-modified mRNA vaccine against all known influenza virus subtypes. *Science* **378**, 899–904 (2022).
37. Harris, A. et al. Influenza virus pleiomorphy characterized by cryoelectron tomography. *Proc. Natl. Acad. Sci. USA* **103**, 19123–19127 (2006).
38. Liu, D.-J. et al. Boost immunizations with NA-derived peptide conjugates achieve induction of NA inhibition antibodies and heterologous influenza protections. *Cell Rep.* **42**, 112766 (2023).
39. Rajendran, M. et al. Analysis of anti-influenza virus neuraminidase antibodies in children, adults, and the elderly by ELISA and enzyme inhibition: evidence for original antigenic sin. *mBio* **8**, 10–1128 (2017).
40. Walz, L., Kays, S. K., Zimmer, G. & von Messling, V. Neuraminidase-Inhibiting antibody titers correlate with protection from heterologous influenza virus strains of the same neuraminidase subtype. *J. Virol.* **92**, 10–1128 (2018).
41. Hovden, A. O., Cox, R. J. & Haaheim, L. R. Whole influenza virus vaccine is more immunogenic than split influenza virus vaccine and induces primarily an IgG2a response in BALB/c mice. *Scand. J. Immunol.* **62**, 36–44 (2005).

42. Moran, T. M., Park, H., Fernandez-Sesma, A. & Schulman, J. L. Th2 responses to inactivated influenza virus can Be converted to Th1 responses and facilitate recovery from heterosubtypic virus infection. *J. Infect. Dis.* **180**, 579–585 (1999).
43. Mozdzanowska, K., Furchner, M., Washko, G., Mozdzanowski, J. & Gerhard, W. A pulmonary influenza virus infection in SCID mice can be cured by treatment with hemagglutinin-specific antibodies that display very low virus-neutralizing activity in vitro. *J. Virol.* **71**, 4347–4355 (1997).
44. Graham, B. S. Rapid COVID-19 vaccine development. *Science* **368**, 945–946 (2020).
45. Kim, K. H. et al. Universal protection against influenza viruses by multi-subtype neuraminidase and M2 ectodomain virus-like particle. *PLoS Pathog.* **18**, e1010755 (2022).
46. Wu, Y. et al. A potent broad-spectrum protective human monoclonal antibody crosslinking two haemagglutinin monomers of influenza A virus. *Nat. Commun.* **6**, 7708 (2015).
47. Margine, I., Palese, P. & Krammer, F. Expression of functional recombinant hemagglutinin and neuraminidase proteins from the novel H7N9 influenza virus using the baculovirus expression system. *J. Vis. Exp*. e51112, https://doi.org/10.3791/51112 (2013).
48. Seephetdee, C. et al. A circular mRNA vaccine prototype producing VFLIP-X spike confers a broad neutralization of SARS-CoV-2 variants by mouse sera. *Antivir. Res.* **204**, 105370 (2022).

Acknowledgements

This work was supported in whole or in part by the National Key R&D Program of China (Grant number: 2022YFC2304204 to Y.-Q.C. 2021YFC2300100 and 2021YFC2300102 to Y.-L.S.), Shenzhen Medical Research Fund: B2302044 to Y.-Q.C., Shenzhen Science and Technology Program (Grant number: JCYJ2020010914243811 to Y.-L.S., JCYJ20190807154603596, KQTD20200820145822023 to Y.-Q.C.). National Natural Science Foundation of China (31970881 and 92169104 to Y.-Q.C.), CAMS Innovation fund for Medical Sciences grant 2022-I2M-1-021 to Y.-L.S. Science and Technology Planning Project of Guangdong Province, China (2021B1212040017). We thank the Experimental Teaching Centre of the School of Public Health (Shenzhen) for providing instrument support for this study.

Author contributions

X.Y., C.Z., S.L., and R.C. designed and performed experiments, analyzed data, and wrote the manuscript. Z.Q., Y.L., X.Z., M.Z., and H.M. assisted in the daily mice weighing. L.L., Y.Z, and W.L. prepared influenza viruses used in the mice challenge experiments. H.L. and Y.W. assisted in analyzing FASC data. Y.S. assisted in recombinant NA purification. M.X., S.L., and K.L. assisted in the format modification. J.L., L.D., Y.L., J.Y., and C.S. supplied critical materials and technical help. All authors reviewed and commented on the manuscript. Y.-Q.C., K.-W.Z., and Y.-L.S. conceived the project, supervised the work, and revised the manuscript.

Competing interests

The authors declare no competing interests.

Declaration of the use of Artificial Intelligence (AI) assisted technology in the manuscript writing

The authors utilized ChatGPT 3.5 to enhance grammar and readability during the manuscript writing. Following this, the authors thoroughly reviewed and edited the article, assuming full responsibility for its content.

Ethics

The Mice experiment proposal was examined and approved by the Institutional Animal Care and Use Committee (IACUC) from the Shenzhen Bay Laboratory. (Ethics File Code: AECYQ202201). Mice experiments were performed according to the animal welfare requirements of Shenzhen Bay Laboratory. Mice influenza virus challenge experiments were performed in the animal biosafety level 2 (ABSL-2) facility at Shenzhen Bay Laboratory.

Additional information

Supplementary information The online version contains supplementary material available at https://doi.org/10.1038/s41541-024-00963-4.

Correspondence and requests for materials should be addressed to Ke-Wei Zheng, Yuelong Shu or Yao-Qing Chen.